

# Simultaneous WDXS and EBSD investigations of dense PLZT ceramics

M. Faryna<sup>a,b,\*</sup>, K. Sztwiertnia<sup>a</sup>, K. Sikorski<sup>c</sup>

<sup>a</sup> Polish Academy of Sciences, Institute of Metallurgy and Materials Science, 25 Reymonta Street, 30-059 Krakow, Poland

<sup>b</sup> Jagiellonian University, Regional Laboratory of Physicochemical Analyses and Structural Research, 3 Ingardena Street, 30-60 Krakow, Poland

<sup>c</sup> Warsaw University of Technology, Faculty of Materials Science and Engineering, Woloska Street 141, 02-507 Warszawa, Poland

Available online 3 April 2006

## Abstract

Electron probe microanalysis (EPMA) with appropriate standards and precisely adjusted experimental conditions has been successfully applied to an accurate quantitative elemental analysis of the lead–lanthanum–zirconium–titanate (PLZT) ceramics with composition  $\text{Pb}_{1-3x/2}\text{La}_x\text{Zr}_{0.65}\text{Ti}_{0.35}\text{O}_3$ , where  $x = 0.08$ . Heterogeneity tests for Pb, La, Ti and Zr performed on highly dense polycrystalline PLZT ceramics showed relatively large scatter in some data, especially for Ti. To check whether the crystallographic orientations or misorientations of PLZT grains have any potential influence on the chemical composition determined by the wavelength-dispersive X-ray spectroscopy (WDXS), orientation maps have been measured, for exactly same areas as in the WDXS measurements. The measurements of single orientations in the PLZT grains were performed with the use of an electron backscatter diffraction (EBSD) facility attached to a low-vacuum scanning electron microscope (LV-SEM). The single orientation maps of the PLZT samples and corresponding WDXS semi-quantitative results for cations concentration distribution are presented and discussed.

© 2006 Published by Elsevier Ltd.

**Keywords:** Electron microscopy; Microstructure; PLZT

## 1. Introduction

Lead–lanthanum–zirconium–titanate (PLZT) solid solution has been widely studied as high-performance ferroelectric material for electro-optical applications (pyroelectric sensors and actuators) as well as for high-speed electrophoretic printing utilizing their memory effect (e.g.<sup>1,2</sup>). Such applications require dense, homogeneous materials with well-defined chemical composition. The PLZT has a perovskite structure, i.e. a simple cubic structure containing three different ions with a general formula of  $\text{ABO}_3$ . The A and B atoms represent +2 and +4 ions, respectively, while the O represents –2 ion. The  $\text{ABO}_3$  structure can be thought of as a face centered cubic (FCC) lattice with A atoms at the corners and the O atoms on the faces. The B atom is located at the center of the lattice. There are minimum energy positions, off centered from the original octahedra that can be occupied by the B atoms. Displacement of this atom by applied electric fields causes the symmetry of the structure to be altered, creating electric dipoles. In PLZT A sites are occupied by La atoms

partially replaced by Pb atoms, while B sites are occupied by Zr atoms partially replaced by Ti atoms.

Electron probe microanalysis (EPMA) with energy-dispersive X-ray spectroscopy (EDXS) and/or wavelength-dispersive X-ray spectroscopy (WDXS) is usually used to determine the chemical composition of PLZT ceramics. However, in the case of  $(\text{Pb},\text{La})(\text{Zr},\text{Ti})\text{O}_3$  solid solution, a quantitative EDXS analysis is not accurate due to the partial overlapping of the ZrL lines with the PbM lines and the TiK lines with the LaL lines. In addition, low concentrations of Ti and La in the material (<5 wt%) reduce the accuracy of the EDXS method. In contrast, WDXS analysis with appropriate standards and precisely adjusted experimental conditions can be used for more accurate quantitative elemental analysis of the PLZT. This is due to superior energy resolution of the crystal spectrometer resulting in significantly higher peak-to-background ratios and better spectral dispersion, thereby minimizing the possibility of peak overlap compared to the EDXS.<sup>3</sup> In the earlier papers<sup>4,5</sup> the composition of highly dense, optically transparent PLZT was determined by use of WDXS. Heterogeneity tests were performed to evaluate the compositional homogeneity of the material and its suitability as a useful reference material for the analysis of other PLZT ceramics and related compounds.

\* Corresponding author. Tel.: +48 12 637 4200; fax: +48 12 637 2192.  
E-mail address: [nmfaryna@imim-pan.krakow.pl](mailto:nmfaryna@imim-pan.krakow.pl) (M. Faryna).

Some compositional inhomogeneity was found inside the PLZT crystals that suggested that the orientation of the grains might influence the chemical analysis.

Most correction procedures applied during EPMA of bulk specimen do not take into account of the crystallographic orientation of the crystal. It has been found that in a transmission electron microscope (TEM) the EPMA results can be influenced by crystal orientation relative to the incident electron beam. This phenomenon has been exploited in the Atom Locations by CHanneling Enhanced MIncroanalysis (ALCHEMI) in the TEM. This quantitative technique, based on differences of the X-ray intensities in different orientations, enables the identification of the crystallographic sites, plus the distribution and types of substitutional impurities in crystals.<sup>6</sup>

The main aim of this paper is to determine if the orientation of a crystal can influence chemical composition obtained during the WDXS analysis of a bulk specimen. Two advanced microscopic techniques, low-vacuum scanning electron microscopy (LV-SEM) equipped with electron backscatter diffraction (EBSD) and EPMA with a WDXS were used.

## 2. Experimental

A specimen of PLZT was prepared by the Ceramics Department of the Jozef Stefan Institute in Ljubljana, Slovenia, by solid-state synthesis and hot pressing. Constituent oxides were mixed according to the formula  $\text{Pb}_{0.92}\text{La}_{0.08}(\text{Zr}_{0.65}\text{Ti}_{0.35})_{1-(0.08/4)}\text{O}_3$ . The powder mixture was calcined at 850 °C, ball milled and heated again to the same temperature. After milling, the powder was cold pressed into a pellet (about 80 mm in diameter and 30–40 mm high) and heated in oxygen at 1200 °C for 2 h. The sample was then heat treated under hot-isostatic pressure for 24 h at 1250 °C. A single phase, fully dense ceramic with PbO-free grain boundaries was obtained. The edges of the bulk specimen were removed. The bulk material was sliced parallel to the diameter producing wafers about 0.5 mm thick and 75 mm in diameter. When carefully polished on both sides, the wafers were optically transparent, which indicated that the PLZT was homogeneous.

The PLZT sample was examined in the LV-SEM to eliminate charging effects usually observed in non-conductive samples. The EBSD hardware was attached to the SEM. Measurements were carried out in a FEI E-SEM XL30 at the acceleration voltage of 20 kV, a tilt angle of 70° and working distance of 16 mm. A special hood has been attached to the SEM pole piece to minimize the so-called “skirt effect” of the primary beam (Fig. 1). This phenomenon is caused by elastic collisions of high-energy electrons with gas molecules in the microscope chamber. The elastic collisions tend to be through relatively large angles and therefore lead to broadening of the electron beam.<sup>7</sup> The backscattered electrons were analyzed and indexed with NORDIF EBSD hardware and CHANNEL 5 EBSD software.

Element concentrations from the points defined in a single run across selected grains of the PLZT sample were analyzed in a CAMECA SEMPROBE SU-30 electron-probe microanalyser equipped with two wavelength dispersive spectrometers. The take-off angle of the instrument was 62°. The intensities of

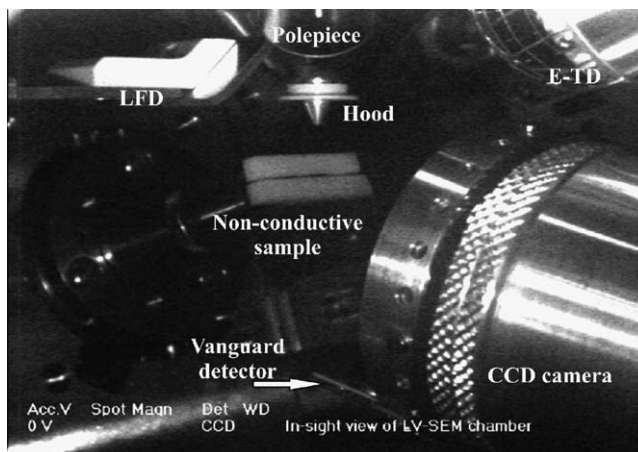


Fig. 1. View of specimen chamber in the VP-SEM with EBSD system attached.

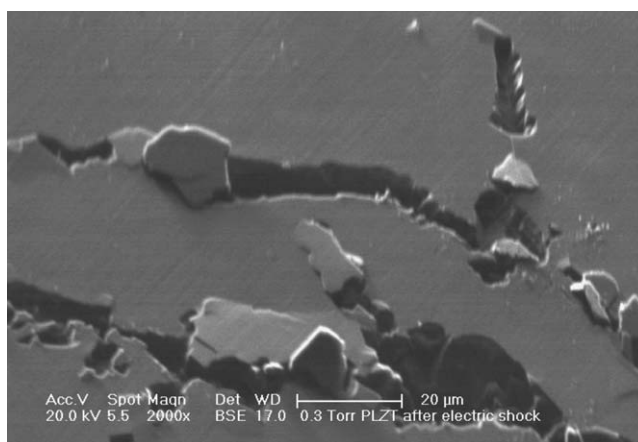


Fig. 2. The surface of PLZT specimen after observations in the conventional SEM.

Pb  $M\alpha_1$ , La  $L\alpha_1$ , Zr  $L\alpha_1$ , Ti  $K\alpha_1$  and O  $K\alpha$  spectral lines of characteristic X-rays were measured at an accelerating voltage  $V = 15$  kV and a beam current  $i = 20$  nA. A PET diffraction crystal was used for the analysis of the spectral lines of Pb, Ti, and La, whereas a TAP crystal was used for Zr and PC2 synthetic

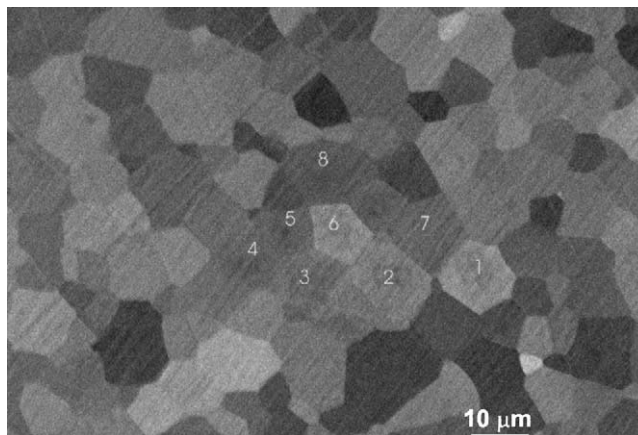


Fig. 3. Backscatter electron image of the polished PLZT sample showing the grains (numbered) from which the WDXS and EBSD measurements were performed.

multilayer crystal for the O K $\alpha$  line. Sphepe (titanite) was used as a standard for Ti and O, LaB $_6$  for La, PbS for Pb and pure Zr for Zr. The concentration of elements was determined from the measured intensities using the commercial computer program, based upon  $\varphi(\rho z)$  correction method.<sup>8</sup>

### 3. Results and discussion

Attempts to observe the PLZT sample without charge neutralization led to charging and destruction of the sample (Fig. 2). The PLZT as a ferroelectric ceramics exhibits spontaneous polarization within the grains. The polarization direction differs from grain to grain and depends on crystallographic orientation. An applied electric field changes the polarization direction leading to mechanical stresses within the grains. If the applied electric field is too strong (and that was the case during conventional SEM observations), it can produce such a large mechanical stress and corresponding strain within the grains that they are pulled out from the matrix leading to crack formation.

The microstructure of the PLZT sample viewed with backscattered electrons is shown in Fig. 3 under LV-SEM conditions. There are clear differences in contrast between the grains caused by electron channelling. The sample was observed in the as-polished condition without any carbon or gold coating. The water vapour pressure was 0.3 Torr, a value sufficient to compensate the electric charge gathered on the sample surface.

The EBSD orientation map recorded in the mode of all Euler angles is shown in Fig. 4. It should be underlined that almost all

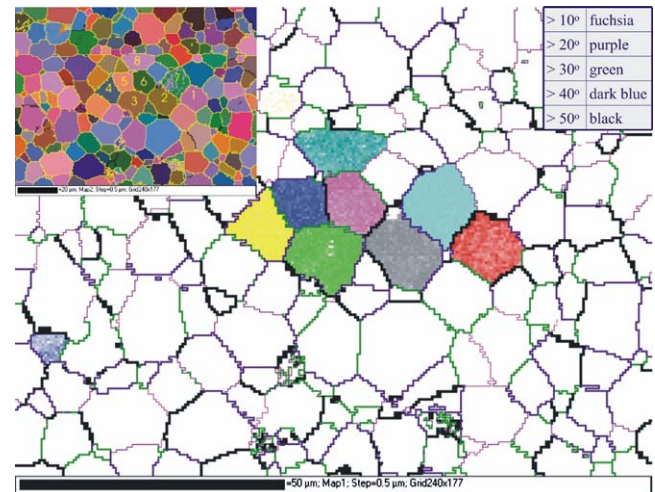


Fig. 4. Euler map with grain boundary distribution.

diffraction patterns (91%) have been solved despite that fact that the investigated material was non-conductive. Only patterns recorded from grain boundaries were not indexed due to overlapping of two patterns from neighbouring grains. However, the problem of non-indexing could be overcome by Zero solution extrapolation. This procedure allows the establishment of a distribution of grain boundaries. The majority of them are high-angle boundaries.

The WDXS measurements were acquired from the eight grains indicated in Fig. 3. The data are given in Fig. 5, where Pb,

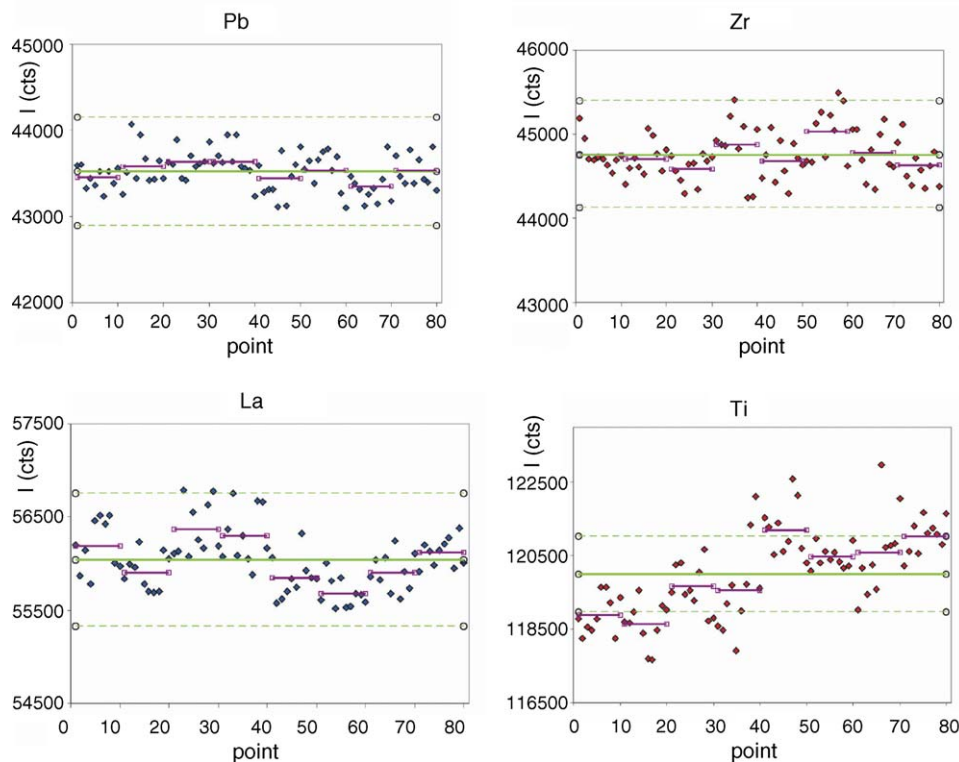


Fig. 5. Variations of cation concentrations in the eight analyzed grains (Pb, Zr, La and Ti intensities vs. analyzed points; scattering range of data is expanded up to three sigma uncertainty); grain 1, points 1–10; grain 2, points 11–20; grain 3, points 21–30; grain 4, points 31–40; grain 5, points 41–50; grain 6, points 51–60; grain 7, points 61–70; and grain 8, points 71–80.

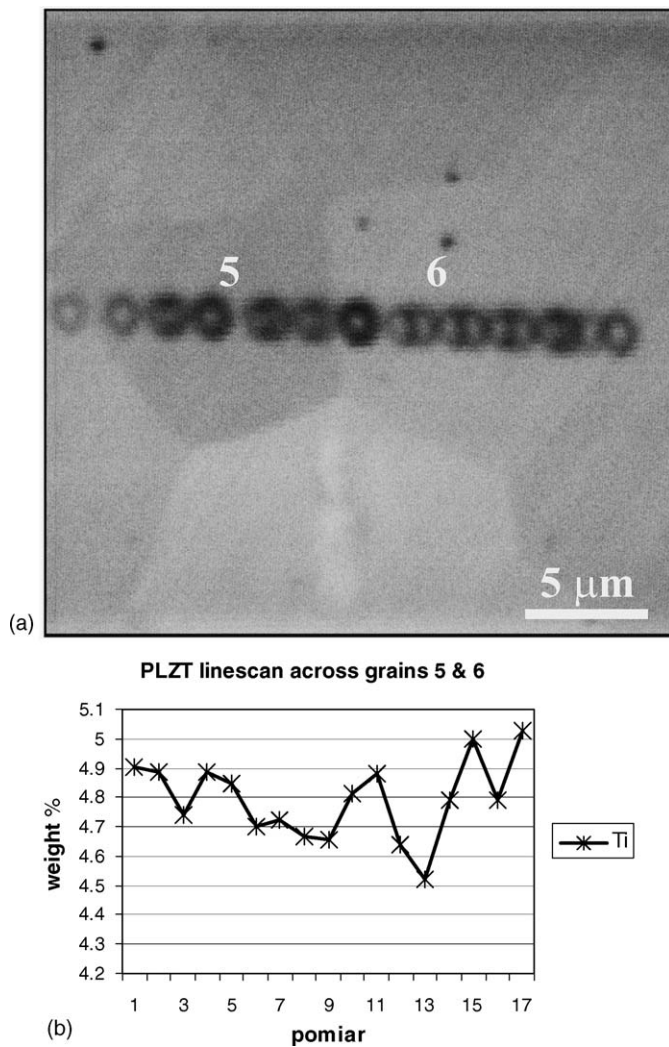


Fig. 6. (a) Backscatter electron image of the grains 5 and 6 (contamination spots indicate the movement of electron beam) and (b) a quantitative WDXS analysis of Ti across the grains 5 and 6.

Zr, La and Ti intensities are plotted versus the analyzed points. The scattering range of the data was expanded up to three sigma uncertainty. Points 1–10 refer to grain 1, points 11–20 to grain 2, points 21–30 to grain 3, etc.

Fig. 5 shows that the content of Pb, La and Zr is reasonably stable and the range of heterogeneity of these cations is minimal in contrast of the Ti content. Fig. 6(a) shows the position of the electron beam during a stepped analysis across grains 5 and 6. The measured Ti concentrations obtained from the analysis in Fig. 6(a) are shown in Fig. 6(b).

The WDXS results shown in Figs. 5 and 6 can be interpreted as follows. The comparison of the average intensities within the grains (sets of 10 measurements) for Ti and Zr revealed a reverse trend in concentrations: the grains with higher Ti concentration contain less Zr atoms and vice versa. Such a situation results, plausibly, in atom exchange at the perovskite B-sites in the PLZT solid solution. Slight variation in the solid solution composition between the grains is generally possible. Thus, the observed changes of Zr/Ti ratio between the grains is in contrast with the

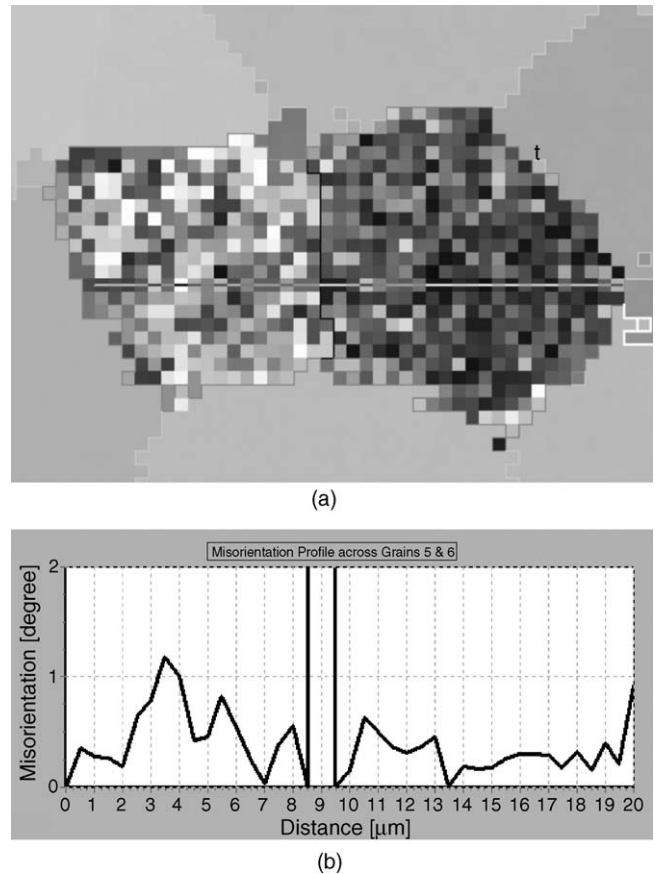


Fig. 7. (a) Orientation map acquired from the grains 5 and 6 (all Euler angles) with the line of misorientation analysis and (b) misorientation profile across the grains 5 and 6 shows the changes of misorientation within the grain.

Pb/La ratio, which remained stable (the distribution of La and Pb seems to be more uniform).

An enlarged image of grains 5 and 6 (Fig. 7) shows the linescan across the crystallites with corresponding misorientations profile. Some changes of misorientations, particularly in the grain 5 (where changes of Ti concentration were also found) can be observed. Though it is rather difficult to judge on this level of investigations whether these two fluctuations have something in common, the presence of such fluctuations and relationship between two signals (Ti  $K\alpha$  intensity and elastically backscatter electrons) has been shown. As the changes of orientation gives a pronounced channeling effect, a very small tilt of crystallographic planes may result in different Ti concentrations recorded by the WDXS.

#### 4. Conclusions

- The LV-SEM makes observation of the PLZT sample in the as-polished condition possible.
- Almost all diffraction patterns (91%) acquired from non-conductive PLZT sample have been successfully indexed.
- Different orientations change the relative intensities of X-ray emission and hence appear to indicate differences in composition.

- There is some evidence of variations of compositions within grains. This can be associated with substitution of Ti atoms by Zr atoms at the perovskite B-sites in the PLZT solid solution.

### Acknowledgements

Financial support from the Polish Committee for Scientific Research (KBN) under contracts No. 62/E-88/SPB/COST/T-08/DWM 121/2004-2005 and No. 134/E-365/SPB/COST/T-08/DWM 124/2004-2005 is gratefully acknowledged.

The authors are grateful to Dr Zoran Samardžija from the JSI, Ljubljana, for supplying the PLZT samples and stimulating discussions.

### References

1. Łoziński, A., Wang, F., Uusimäki, A. and Leppävuori, S., PLZT thick films for pyroelectric sensors. *Meas. Sci. Technol.*, 1997, **8**, 33–37.
2. Hirt, A., Printing with ferroelectric ceramics. *Ferroelectrics*, 1997, **201**, 1–11.
3. Goldstein, J., Newbury, D., Joy, D., Lyman, Ch., Echlin, P., Lifshin, E. et al., *Scanning Electron Microscopy and X-Ray Microanalysis*. Kluwer Academic/Plenum Publishers, New York, 2003, pp. 340–346.
4. Marinienko, R. B., Samardžija, Z., Bernik, S., Čeh, M. and Kosec, M., Evaluation of a lead lanthanum zirconium titanate (PLZT) specimen for use as an electron microprobe reference material. *Proc. Microsc. Microanal.*, 2001, **7**(Suppl. 2), 680–681.
5. Bernik, S., Marinienko, R. B., Holc, J., Samardžija, Z., Čeh, M. and Kosec, M., Compositional homogeneity of ferroelectric (Pb,Lu)(Ti,Zr)O<sub>3</sub> thick films. *J. Mater. Res.*, 2003, **18**, 515–523.
6. Spence, J. C. H. and Taftø, J., ALCHEMI: a new technique for locating atoms in small crystals. *J. Microsc.*, 1983, **130**, 147–154.
7. Donald, A. M. and Thiel, B. L., ESEM contrast and applications to wet organic materials. In *Impact of Electron and Scanning Probe Microscopy on Materials Research, NATO ASI series*, ed. D. G. Rickerby. Kluwer Academic/Plenum Publishers, New York, 1999, pp. 415–444.
8. Pouchou, J. L. and Pichoir, F., Quantitative analysis of homogeneous or stratified microvolumes applying the model “PAP”. In *Electron Probe Quantitation*, eds. K. F. J. Heinrich and D. E. Newbury. Plenum Press, New York, 1991, pp. 31–75.